Diffractive Physics at HERMES

A. Borissov[a](for the HERMES Collaboration)

[a]Physics Department, 2477 Randall Laboratory, The University of Michigan, Ann Arbor, MI 48109-1120,USA.

The measured decay angle distributions of the ρ^0 are in agreement with the hypothesis that the reaction is dominated by helicity conserving amplitudes with natural parity exchange, and are used to extract a measure of $R \equiv \sigma_L/\sigma_T$. Cross section measurements of exclusive ρ^0 production on ${}^1H$ and ${}^3He$ targets in the range $0.5 < Q^2 < 5.6$ GeV^2 as well as extrapolated photoproduction cross section are presented in comparison with world data. The Q^2-dependence of the cross section is well described by the propagator originating from the Vector Meson Dominance model with a power dependence of 2.5. The observed $W-$dependence is described by a model based on Regge field theory. A perturbative QCD calculation based on Off-Forward Parton Distributions also gives a good description of the longitudinal component of the cross section for $Q^2 > 2$ GeV^2.

1. INTRODUCTION

HERMES is an internal gas target experiment located in the East Hall of the HERA storage ring complex at DESY. The HERMES spectrometer [1] has been constructed with acceptance sufficient to allow the detection of scattered leptons in coincidence with quark fragmentation products. It consists of two identical halves having acceptance $40 < \Theta < 220$ mrad with momentum resolution $\leq 1\%$, and identification of electrons with efficiency $> 97\%$ at hadron contamination $< 1\%$.

The ρ^0, ϕ, ω and J/ψ mesons are identified by their decay products in the following channels: $\rho^0 \rightarrow \pi^+\pi^-(100\%)$, $\omega \rightarrow \pi^+\pi^-\pi^0$; $\pi^0 \rightarrow \gamma\gamma(88\%)$, $\phi \rightarrow K^+K^-(49\%)$, $J/\psi \rightarrow e^+e^-, \mu^+\mu^-(6\% + 6\%)$. The numbers in brackets indicate the branching ratios. Approximate numbers of detected elastic events in the years 1995-1997 are: $\rho^0 \sim 12000$, $\omega \sim 500$, $\phi \sim 1200$. About 120 J/ψ have been reconstructed, without the separation of different production mechanisms because the scattered positron was usually not detected for these events.

Exclusive ρ^0 production in deep inelastic scattering was analysed in terms of angular distributions, cross sections, and the observation of a coherence length effect [2]. Events corresponding to exclusive diffractive ρ^0 production were extracted from the data which contained a scattered positron and two hadrons with opposite charge. Subsequently a number of geometric cuts were imposed on the particle tracks to ensure that they were well contained within the acceptance of the spectrometer. The ρ^0 mesons are identified by requiring $0.6 < M_{\pi\pi} < 1$ GeV, with $M_{\pi\pi}$ being the invariant mass of the two detected hadrons assuming that both are pions. The $\phi \rightarrow K^+K^-$ background was removed by the requirement of $M_{KK} > 1.04$ GeV.

Non-exclusive background was removed principally by the requirement of missing energy $-2 < \Delta E < 0.6(0.4)$ GeV for the ${}^3He$ (${}^1H$) data. The remaining background ($\sim 10\%$) was subtracted from the ${}^1H$ data using a Monte Carlo calculation of pions from deep-inelastic scattering and from non-diffractive vector meson production. In the ${}^3He$ case, the background was determined by constructing a ΔE spectrum for $0.7 < -t' < 5$ GeV^2, i.e. well beyond the diffraction region. The data were corrected for the finite acceptance of the spectrometer.

2. ANGULAR DISTRIBUTIONS

The extraction of matrix elements from the measured angular distributions of diffractive ρ^0 production at HERMES allows the testing of s-channel helicity conservation (SCHC) and natural parity exchange [3]. A detailed review of this type of analysis can be found in [4].

Briefly, if SCHC is valid and if the $t-$channel exchange particle in a diffractive exclusive ρ^0 production reaction has natural parity $P = (-1)^J$, then the matrix elements r^{04}_{00} and r^1_{1-1} extracted from the measured distributions should be correlated: $r^1_{1-1} = \frac{1}{2}(1 - r^{04}_{00})$. These are derived from fits of two angular distributions: the angle θ, which is the polar angle between the positive decay pion and the ρ^0, and the difference $\Psi \equiv \phi - \Phi$, where ϕ is the angle between the ρ^0 decay and production planes and Φ is the angle between the lepton scattering and ρ^0 production planes. The expected correlation is observed, allowing one to conclude that HERMES data are consistent with SCHC and natural parity exchange.

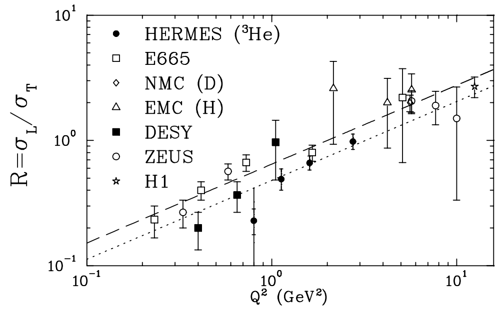

Figure 1. The ratio R_ρ is shown (full circles, with statistical errors only). Previous measurements (with statistical errors only) from DESY, NMC, EMC, ZEUS and H1 are shown for comparison.

The measured spin density matrix elements can be used to determine the Q^2 dependence of the ratio of longitudinal to transverse ρ^0 production cross sections $R \equiv \sigma_L/\sigma_T = \frac{1}{\epsilon}\frac{r^{04}_{00}}{1-r^{04}_{00}}$. Here ϵ is the virtual photon polarization parameter [4]. Results for $R(Q^2)$ are presented in fig. 1. The world data are fit to the form:

$$R(Q^2) = c_0(W) \cdot \left[\frac{Q^2}{M^2_\rho}\right]^{c_1}. \qquad (1)$$

The fit yields the values $c_1 = 0.63 \pm 0.04$, $c_0 = 0.46 \pm 0.03$ for the data from high energy muon beams and collider experiments spanning $6 < W < 140\,\mathrm{GeV}$ (EMC, NMC, E665, ZEUS, and H1), and $c_0 = 0.34 \pm 0.03$ for data with lower beam energy covering $2 < W < 6.5\,\mathrm{GeV}$ (DESY and HERMES). The Q^2 dependence of R is consistent with previous experiments, exhibiting a monotonic increase with Q^2 and marked disagreement with the VDM prediction $c_1 \equiv 1$ [5]. In addition, the HERMES data taken together with low energy data from DESY and compared with world data at higher energy suggest enhanced transverse strength at lower energy for fixed Q^2.

3. CROSS SECTION

Exclusive cross sections have been measured for W values between 4.0 and 6.5 GeV, and Q^2 values between 0.6 and 5.6 GeV^2, from both ^{1}H and ^{3}He targets. For the measurement of the virtual photoproduction cross section, several corrections were taken into account: the photon flux factor, radiative corrections ($\sim$ 15% for ^1H and $\sim$ 20% for ^3He), subtraction of the double diffractive contribution ($\sim$ 5%), and coherent and nuclear transparency corrections in the case of ^3He data [2,6]. In fig. 2 the virtual photoproduction cross section is plotted versus W, and compared to existing measurements [7–12] at nearby values of W. As data from both targets are mutually consistent, henceforth only the ^1H data will be discussed.

The Q^2 dependence of the cross section has been parametrized using the following form, which has been taken from the Vector Dominance Model (VDM) [5,11]:

$$\sigma(Q^2) = \sigma(Q^2=0) \cdot \left(\frac{m^2_\rho}{Q^2 + m^2_\rho}\right)^m \cdot (1 + \epsilon R_\rho). (2)$$

Here $R_\rho = \xi^2 Q^2/m^2_\rho$ represents the ratio of longitudinal and transverse ρ^0 production cross sections. A good description of the data is obtained setting $m = 2$ and treating $\sigma(Q^2 = 0)$ and ξ^2 as free parameters. The results of this fit are presented in the first half of table 1.

As the ratio R must be positive, the negative fit values for ξ^2 indicate a deficiency of Eq. 2.

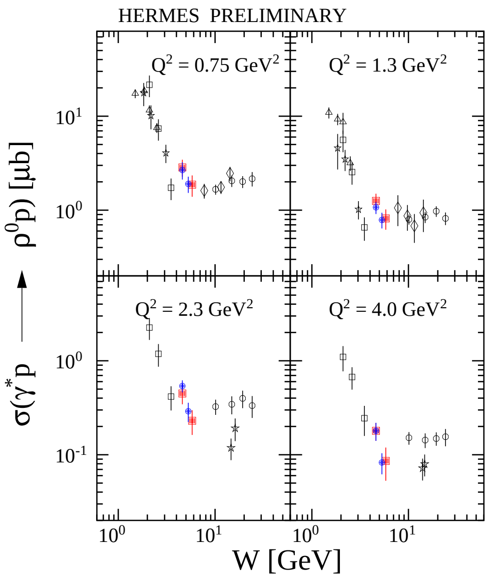

Figure 2. The virtual photoproduction cross section for ρ^0 production versus W for the indicated values of average Q^2. The HERMES data are represented by solid circles (^1H) and solid squares (^3He). The open squares are from [7], open triangles [8], open stars [9], open diamonds [10], open circles [11], closed stars [12]. The error bars include both the statistical and systematic uncertainties added in quadrature.

Hence the exponent m of the propagator was used as a free parameter while the value of R_ρ was taken from measurements of decay angle distributions (eq. 1). The results listed in the second half of table 1 quantitatively confirm similar conclusions obtained by the E665 collaboration ($m = 2.51 \pm 0.07$ at $W \approx 15$ GeV) [11]. The fitted value of the extrapolated photoproduction cross section σ_0 are taken from the first fit (following [11]), and are in agreement with world data as shown in fig. 3.

In fig.4 the ρ^0 electroproduction data are compared with Regge based calculations of [14] which relate the $W-$dependence of vector meson production to the proton structure function $F_2^p(x, Q^2)$. The HERMES data are found to be in reasonable agreement with this model.

Table 1
The fitted photoproduction cross sections from ^{1}H data. Both statistical and systematic uncertainties were included at fitting procedure.

$< W >, GeV$	$\sigma(Q^2 = 0)$ (μb)	ξ^2
4.6	12.11 ± 2.35	-0.02 ± 0.06
5.4	9.96 ± 1.71	-0.12 ± 0.040
$< W >, GeV$	$\sigma_(Q^2 = 0)$ (μb)	m
4.6	12.38 ± 3.79	2.39 ± 0.22
5.4	14.96 ± 4.86	2.83 ± 0.24

In order to compare the data to the new OFPD calculations of ref.[15], the longitudinal component σ_L has been determined according to [4] with R_ρ taken from the HERMES angular distributions (eq. 1), see fig. 5. It is interesting to note that the calculations qualitatively reproduce the observed rise of the cross section at low W, which is presumably associated with the valence quark contribution.

4. OVERLOOK

The data collected at HERMES on exclusive diffractive ρ^0 production allow one to conclude that the Vector-Dominance Model is not applicable in the kinematic domain of the experiment. From the W dependence of the cross section, it follows that Pomeron exchange mechanism is strongly suppressed. The HERMES data thus appear to lie in the transition energy region where the quark exchange mechanism becomes dominant over gluon exchange, at least for the longitudinal component of the cross section.

REFERENCES

1. K.Ackerstaff et al, preprint DESY 98-057, hep-ph/9806008.
2. K. Ackerstaff et al.(HERMES), Phys. Rev. Lett. **82** (1999) 3025, hep-ex/9811011.
3. K. Schilling and G. Wolf, Nucl. Phys. **B61** (1973) 381.

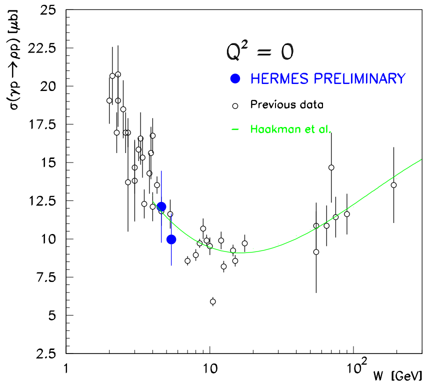

Figure 3. The extrapolated HERMES data (closed symbols) for σ_0 are compared with direct measurements (open symbols) from [13]. The curve represents the results of a calculation by L.Haakman et al [14].

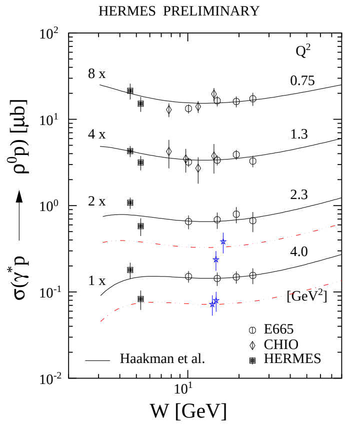

Figure 4. The virtual photoproduction cross section versus W at the indicated average Q^2 values. The symbols used have the same meaning as in fig. 2; the closed stars are NMC data. The lines represent the calculation of [14] normalized to E665 (solid) or NMC (dashed) data.

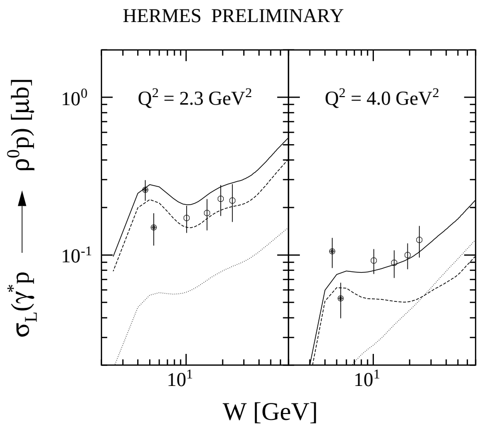

Figure 5. The longitudinal component of the virtual photoproduction cross section versus W at average Q^2 values 2.3 and 4.0 GeV^2. The symbols used have the same meaning as in fig. 2. The solid lines represent the results of the OFPD calculations of [15]. The dashed (dotted) curves represent the quark (2-gluon) contributions.

4. J.A. Crittenden, preprint DESY 97-068, BONN-IR-97-01 (1997).
5. T.H. Bauer et al., Rev. Mod. Phys. **50** (1978) 261.
6. M.Kolstein PhD Thesis, Vrije Universiteit, Amsterdam (1998), unpublished.
7. D.G.Cassel et al.,Phys.Rev. **D24** (1981) 2787.
8. P.Joos et al., Nucl.Phys. **B113** (1976) 53.
9. del Papa et al., Phys.Rev. **D19** (1979) 1303.
10. W.D. Shambroom et al.,Phys. Rev. **D26** (1982).
11. M.R.Adams et al. (E665),Z.Phys. **C74** (1997) 237.
12. M. Areneodo et al.(NMC),Nucl.Phys. **B429** (1994) 503.
13. Eur.Phys. J. **C2** (1998) 247.
14. L.P.A.Haakman, A.Kaidalov, J.H.Koch, Phys.Lett. **B365** (1996) 411.
15. M.Vanderhaeghen, P.A.M. Guichon, M. Guidal, Phys.Rev.Lett. **80** (1998) 5064.